MECHANICS OF OBLIQUE MACHINING: PREDICTING CHIP GEOMETRY AND CUTTING FORCES FROM WORK MATERIAL PROPERTIES AND CUTTING CONDITIONS

G. C. I. Lin, PhD* Professor P. L. B. Oxley, BSc, PhD, CEng, MIMechE†

An approximate theory of oblique machining is obtained by assuming that the plastic deformation in the plane normal to the cutting edge is equivalent to the flow in orthogonal machining. Equations are derived from which the chip geometry, including the direction of chip flow, and the three components of cutting force can be calculated for given cutting conditions and material properties. Results of machining tests are used to calculate the flow stress properties of the work material which are then used with the oblique machining theory to predict forces etc. Predicted and experimental results are shown.

1 NOTATION

C Constant in strain-rate equation.
F Frictional force at tool–chip interface.
F_C Force component in direction of cutting.
F_R Force component normal to F_C and F_T.
F_S Shear force.
F_T Force component normal to direction of cutting and machined surface.
i Inclination angle.
k Shear flow stress.
k_{AB} Shear flow stress on plane AB.
l Length of AB.
N Normal force at tool–chip interface.
n Strain-hardening exponent.
P Force component normal to normal plane.
R Resultant cutting force.
t_1 Depth of cut.
t_2 Chip thickness.
U Cutting velocity.
V Chip velocity.
V_s Shear velocity.
w Width of cut.
α Tool rake angle.
α_e Effective rake angle.
γ Shear strain.
γ_{AB} Shear strain at AB.
$\dot{\gamma}$ Shear strain rate.
$\dot{\gamma}_{AB}$ Shear strain rate at AB.
ϵ Uniaxial strain.
ϵ_{AB} Strain at AB.
$\dot{\epsilon}$ Uniaxial strain rate.
η Chip flow angle.
θ Angle between resultant cutting force and AB.
λ Friction angle.
σ Uniaxial stress.
σ_{AB} Flow stress at AB.
σ_1 Constant in equation (5) (flow stress at $\epsilon = 1$).
ϕ Shear angle.

Subscript n and prime denote normal plane values.

This paper is published for written discussion. The MS. was received on 17th August 1971 and accepted for publication on 6th April 1972. 22

* *Teaching Fellow, School of Mechanical and Industrial Engineering, University of New South Wales.*
† *Sir James Kirby Professor of Production Engineering, School of Mechanical and Industrial Engineering, University of New South Wales.*

2 INTRODUCTION

INVESTIGATIONS OF THE MECHANICS of machining are usually limited to the relatively simple case of machining with a single straight cutting edge which is set parallel to the surface being machined and normal to the cutting velocity, i.e. the angle i in Fig. 1 is zero and is the angle between the cutting velocity and the normal to the cutting edge measured in the plane of the machined surface. This process is termed orthogonal machining and if the depth of cut t_1 (Fig. 1) is small compared with its width w then the removed chip is formed under approximately plane-strain conditions with no flow in a direction parallel to the cutting edge. The chip flows across the tool cutting face in a direction normal to the cutting edge and the complete chip formation process can be represented in two dimensions (Fig. 2). The theory of plane strain, plastic flow, is relatively well understood and it is for this reason that investigations have been concentrated on orthogonal machining. However, it is only recently that an adequate theory has been obtained for this case.

Although many practical machining processes are approximately orthogonal they could often be represented more accurately by a chip formation model in which the angle i is not zero and the cutting edge is inclined to the cutting velocity as shown in Fig. 1. This process, which is

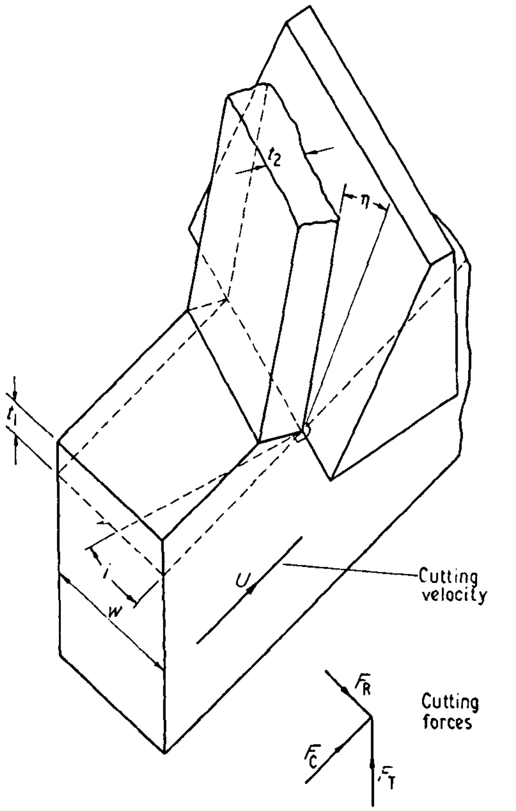

Fig. 1. Model of oblique machining process

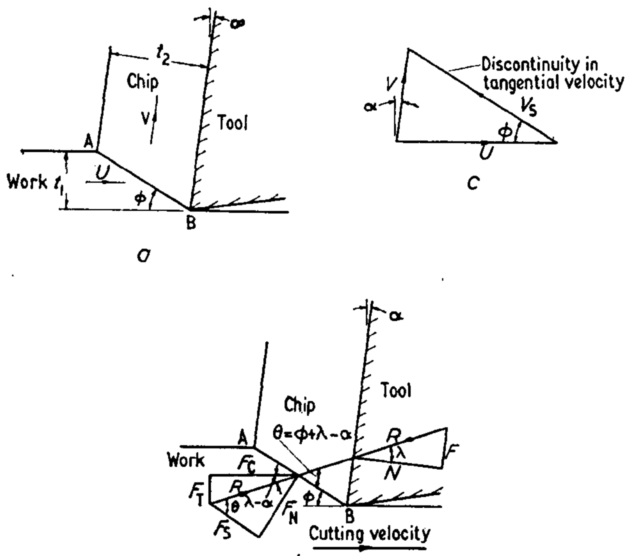

Fig. 2. Model of orthogonal chip formation used in analysis: (*a*) Chip formation, (*b*) Force diagram (*c*) Velocity diagram.

known as oblique machining, is three-dimensional and the chip flow direction is inclined at an angle η (Fig. 1) to the normal to the cutting edge where η is measured in the plane of the cutting face. It is not apparent from geometry what the value of η should be.

Considering the extreme difficulty of analysing three-dimensional plastic flow problems it is not surprising that to date there has been no analysis of oblique machining comparable to those for the orthogonal case. On the other hand the various geometric relations between cutting forces and overall chip geometry are as well established for oblique as for orthogonal machining. Also, a number of empirical equations have been obtained for the cutting forces, chip-flow direction etc. in oblique machining. One of these is the well-known 'flow rule' of Stabler (1)*, that is

$$\eta = i \quad . \quad . \quad . \quad . \quad . \quad (1)$$

where η and i are measured in the same sense from their respective normals to the cutting edge as shown in Fig. 1. Equation (1) has been found to give good agreement with experimental results over a wide range of cutting conditions.

It is well known from experiment that the slope of the tool cutting face relative to the cutting velocity is one of the most important parameters in determining cutting forces etc. In orthogonal machining this slope is defined by a single angle, the rake angle, α (Fig. 2), where α is the angle between the cutting face and the normal to the cutting velocity measured in the plane normal to the cutting edge. In oblique machining it is not obvious which slope should be considered. For example it could be the angle between the cutting face and the normal to the cutting velocity measured in the plane containing the cutting velocity and chip velocity which is sometimes called the effective rake angle α_e. Alternatively, it could be the so-called normal rake angle α_n measured in the plane normal to the cutting edge as in orthogonal machining. Experiments (2) in which α_n and α_e were in turn held constant while the inclination angle i was varied showed little variation in the cutting force in the cutting velocity direction for constant α_n but large variation for constant α_e. From these results, therefore, it might be concluded that α_n is the rake angle most directly related to the process. An excellent account of experimental and analytical investigations of oblique machining is given in the book by Armarego and Brown (3).

In the analysis of oblique machining described in this paper it is assumed that the flow in the plane normal to the cutting edge can be treated as plane strain deformation as in orthogonal machining. By making further assumptions this flow is then related to the actual three-dimensional process.

3 THEORY

3.1 Orthogonal

The analysis is based on the model of chip formation shown in Fig. 2. The process is assumed to be steady state with the chip formed by plastic deformation with no cracks occurring in the deforming material and with no build-up of material on the tool cutting edge. It is further assumed that the deformation is plane strain with planes normal to the cutting edge being typical planes of flow.

In the shear plane model of chip formation the chip is assumed to be formed by shear along a straight shear plane AB (Fig. 2) which represents the finite plastic zone in which the chip is actually formed in practice. With this model work material approaches the shear plane with the cutting velocity U which is changed instantaneously at AB to the chip velocity V. The chip velocity is constant across the chip and the well-known tendency for the chip to curl

* *References are given in the Appendix.*

is neglected. The instantaneous change in velocity at AB requires a discontinuity in the tangential velocity along AB as shown by the velocity diagram in Fig. 2. This is quite acceptable from the viewpoint of continuity, i.e. volume constancy, but is only acceptable for stress if the work material can be assumed to be rigid–plastic and to deform with constant flow stress. It has been shown (4) that this last point greatly restricts the value of theories based on the shear plane model.

Slip-line fields constructed (5) (6) from experimentally observed flow fields have shown that the family of slip-lines running from the tool cutting edge to the work–chip free surface are approximately straight near the centre of the field. If the construction in Fig. 2 is used with the experimental flow fields to locate AB it is found that AB approximates closely to one of the straight slip-lines. It is therefore possible to use the model of chip formation in Fig. 2 with AB representing a straight slip-line near the centre of a finite slip-line field in which there is no velocity discontinuity. The overall change in velocity can still be represented by the velocity diagram in Fig. 2 but with V_s now representing the total change in velocity which occurs in the plastic zone in the direction of AB. As a slip-line AB can be assumed to be a direction of maximum shear stress and of maximum shear strain-rate and by analysing the stresses along AB it is possible to derive equations for predicting chip geometry, cutting forces, etc. With this model it is no longer necessary to assume that the work material deforms with constant flow stress and far more reasonable assumptions can be made. This is the approach used in a number of recent papers (4) (7) including the present one. The theory has been described previously (4) (7), but in the description which follows the approach is somewhat different.

For a given depth of cut t_1 (Fig. 2) and rake angle, α, the geometry of Fig. 2 is not completely specified unless either the chip thickness t_2 or the shear angle ϕ (the angle between AB and the cutting velocity) is known. Without ϕ (or t_2) no estimates can be made of cutting forces, etc. A theory for predicting ϕ in terms of known parameters is therefore sought.

In a recent investigation (8) printed grids were used to obtain records of the flow in orthogonal machining and from these distributions of maximum shear strain-rate along streamlines of flow were calculated. These showed that the maximum value of the maximum shear strain-rate occurred near to AB with the distribution of strain-rate more or less symmetrical about AB. For a given set of cutting conditions this maximum value was approximately constant along AB, although near the cutting edge it tended to increase. The results show that for a very wide range of cutting conditions the shear strain-rate along AB, $\dot{\gamma}_{AB}$, can be estimated from the equation

$$\dot{\gamma}_{AB} = C\frac{V_s}{l} \quad . \quad . \quad . \quad . \quad (2)$$

where C is a constant for a particular material; V_s (in s^{-1}) is the shear velocity which is equal to the velocity discontinuity found from the velocity diagram in Fig. 2, i.e. $V_s = 0{\cdot}2\, U \cos\alpha/\cos(\phi-\alpha)$; U (ft/min) is the cutting velocity and l (in) is the length of AB (i.e. $l = t_1/\sin\phi$). The symmetry of the strain-rate distribution about AB means that approximately half of the total strain occurring in the plastic zone has taken place by the time the material reaches AB, therefore the shear strain at AB, γ_{AB}, can be estimated from the equation

$$\gamma_{AB} = \frac{1}{2}\frac{\cos\alpha}{\sin\phi\cos(\phi-\alpha)} \quad . \quad . \quad (3)$$

If the cutting tool is sharp then AB transmits the resultant cutting force R (Fig. 2) which is also transmitted across the tool–chip interface. The inclination of the resultant cutting force to AB can therefore be found by analysing the stresses acting on AB. The shear stress along AB will be the maximum shear stress in plane strain (shear flow stress) and the normal stress on AB will be the hydrostatic stress. It is reasonable to assume that the strain, strain-rate and temperature are constant along AB and therefore that the shear flow stress along AB is constant. The distribution of hydrostatic stress along AB can be determined by considering the equilibrium of a small element at the free surface at A and then applying the appropriate stress equilibrium equation along AB. By combining these stress distributions it can be shown that

$$\tan\theta = 1+2\left(\frac{\pi}{4}-\phi\right)-Cn \quad . \quad . \quad (4)$$

where θ (Fig. 2) is the angle between the resultant force and AB; ϕ is the shear angle; C is the constant in equation (2) and n is the strain-hardening exponent in the equation

$$\sigma = \sigma_1\epsilon^n \quad . \quad . \quad . \quad . \quad . \quad (5)$$

This equation is used to represent the flow stress characteristics of the work material. In equation (5) σ and ϵ are the uniaxial stress and strain and the constants σ_1 and n will in general be functions of strain-rate and temperature. It should be noted that in deriving equation (4) it has been assumed that the flow stress gradient normal to AB results from strain-hardening only and that the influence of the temperature gradient across AB is negligible. The derivation of essentially the same equation as equation (4) is given in reference (7). By considering the force diagram in Fig. 2 it can also be shown that

$$\theta = \phi+\lambda-\alpha \quad . \quad . \quad . \quad . \quad (6)$$

where λ is the average friction angle along the tool–chip interface, that is

$$\tan\lambda = \frac{F}{N} \quad . \quad . \quad . \quad . \quad (7)$$

F and N (Fig. 2) are the friction and normal forces acting at the tool–chip interface.

It can now be seen that equations (4) and (6) are sufficient to calculate ϕ if the appropriate values of C, n, α and λ are known. Once ϕ is known then the corresponding forces F_C (Fig. 2) in the cutting velocity direction and F_T normal to this direction can be found from the equations

$$\left.\begin{aligned} F_C &= \frac{t_1 w k_{AB}\cos(\lambda-\alpha)}{\sin\phi\cos(\phi+\lambda-\alpha)} \\ &\text{and} \\ F_T &= \frac{t_1 w k_{AB}\sin(\lambda-\alpha)}{\sin\phi\cos(\phi+\lambda-\alpha)} \end{aligned}\right\} \quad . \quad . \quad (8)$$

t_1 and w are the depth and width of cut and k_{AB} is the shear flow stress along AB. k_{AB} is found from equation (5) using the value of strain given by equation (3). If σ_1 and n

are taken as functions of strain-rate then the appropriate strain-rate is found from equation (2). In relating uniaxial and plane strain conditions the relations based on the shear strain energy yield criterion are used.

$$\left.\begin{aligned} k &= \frac{\sigma}{\sqrt{3}} \\ \gamma &= \sqrt{3}\,\epsilon \\ \dot{\gamma} &= \sqrt{3}\,\dot{\epsilon} \end{aligned}\right\} \quad . \quad . \quad . \quad . \quad (9)$$

3.2 Oblique

To obtain a theory of oblique machining one possible approach is to assume that the flow in the plane normal to the cutting edge can be analysed as if it is orthogonal (plane strain) flow. This is clearly an approximation as there will be flow normal to this plane, i.e. parallel to the cutting edge. The smaller the inclination angle i the better this approximation should be. An alternative approach would be to consider the flow in the plane containing the cutting velocity and chip velocity as equivalent to orthogonal flow. In this case there is no flow normal to the plane but the normal stress on AB does not act in a direction parallel to the plane. Preliminary trials using both approaches showed that the analysis based on the normal plane was the more promising.

The cutting forces in oblique machining can be expressed in terms of three mutually perpendicular components F_C, F_T and F_R, where the positive directions of the forces acting on the tool are taken as shown in Fig. 1. F_C is the force in the cutting velocity direction, F_T the force normal to the machined surface and F_R the force normal to the other two forces. The resultant of these three components can be resolved into a component R' in the normal plane and a component P normal to this plane. It is now assumed that the orthgonal analysis given above applies to the normal plane with the resultant R' replacing R. In using the orthgonal equations all the forces are replaced by equivalent forces represented with a prime, thus F_C becomes F'_C and so on. The prime notation is also used with the velocities and the dimensions of the cut. To keep in line with previous work the subscript n is used with angles, for example ϕ_n is the normal shear angle. It should be noted that if U and w (Fig. 1) are the cutting velocity and width of cut then $U' = U \cos i$ and $w' = w/\cos i$. The depth of cut ($t'_1 = t_1$) and chip thickness ($t'_2 = t_2$) are unchanged. For given values of C, n, α_n, λ_n and i the modified equations can now be used to calculate ϕ_n and hence, if σ_1 in equation (5) is known, F'_C and F'_T.

To relate the flow in the normal plane to the complete flow the following assumptions have to be made:

(1) that the resultant frictional force ($\bar{P}+\bar{F}'$) on the tool face will act in the direction of the chip velocity

(2) that the resultant shear force ($\bar{P}+\bar{F}'_S$) on the plane defined by ϕ_n will act in the resultant shear velocity direction where this is defined by the velocity diagram (Fig. 2) constructed in the plane containing the cutting velocity and chip velocity.

The satisfaction of these two conditions determines the chip flow direction with η given by the equation

$$\tan \eta = \frac{\tan i \cos \alpha_n}{\tan (\phi_n + \lambda_n)} + \sin \alpha_n \tan i \quad . \quad (10)$$

This equation was derived by Stabler (1) who used it in conjunction with his empirical 'flow rule', i.e. equation (1), to obtain the shear-angle relation

$$\phi_n = \frac{\pi}{4} + \frac{\alpha_n}{2} - \lambda_n \quad . \quad . \quad . \quad (11)$$

In general this does not give a good fit with experimental results. The approach in the present analysis is to find ϕ_n by the method described above and then to use equation (10) to calculate η. Once η is known then the three components of cutting force (Fig. 1) can be calculated from the equations

$$\left.\begin{aligned} F_C &= F'_C \cos i + P \sin i \\ F_T &= F'_T \\ F_R &= F'_C \sin i - P \cos i \end{aligned}\right\} \quad . \quad . \quad (12)$$

P is given by

$$\begin{aligned} P &= F' \tan \eta \\ &= [(F'_C)^2 + (F'_T)^2]^{1/2} \sin \lambda_n \tan \eta \quad . \quad (13) \end{aligned}$$

For given values of α_n, λ_n and i together with the appropriate material properties, i.e. C in equation (2) and σ_1 and n in equation (5) it is now possible to calculate ϕ_n, η and the three components of cutting force F_C, F_T and F_R.

4 EXPERIMENT

A series of orthogonal and oblique machining tests were made on a lathe to obtain experimental results suitable for checking the theory developed in the previous section. The experimental method and equipment will be described fully in another paper (9) and only a brief description is given here. An undercutting tool was used to produce a short length of tube at the end of a solid round bar. The tests were then made by reducing the length of the tube with a straight edge cutting tool (brazed sintered carbide) with the cutting edge normal to the feed direction. For the orthogonal tests the cutting edge was set normal to the cutting velocity, which for the small feed used was taken as the work velocity, while for the oblique tests it was inclined to this velocity. The tube thickness, equivalent to the width of cut w (Fig. 1), was maintained at 0·2 in ± 0·003 in. This was sufficient to give approximately plane strain conditions in the orthogonal tests and yet small enough to give only a small velocity gradient across the width with a workpiece outside diameter of 5·85 in. In each test a tube length of 0·25 in was produced and this was found sufficient to enable steady cutting conditions to be achieved and cutting forces recorded. The work material was S1214 steel (Australian specification) which is a free machining steel (0·084 per cent C, 0·28 per cent S, < 0·01 per cent Si, 0·064 per cent P, 0·94 per cent Mn, < 0·1 per cent Cu). This was obtained in the form of 6 in diameter cold rolled bright bar and used in the as-received condition. With this material a continuous chip with no built-up edge was produced over the range of cutting conditions used. These were cutting velocity U of 25, 200, 400, 600, 800 and 1000 ft/min; width of cut w, 0·2 in; depth of cut (feed) t_1, 0·019 24 in; normal rake angle α_n (α in orthogonal tests), 20°; and inclination angle i, 0°, 10°, 20° and 30°.

The experimental results and some results derived from these are given in Table 1. The cutting velocity U was found from the spindle rotational speed measured using an accurate tachometer and the measured mean diameter of

Table 1. Experimental results

Rake angle $\alpha_n = \alpha = 20°$. Depth of cut $t_1 = 0{\cdot}019\,24$ in.

i, degrees	U, ft/min	lbs			η, degrees	λ_n and λ, degrees	ϕ_n and ϕ, degrees
		F_C	F_T	F_R			
30	25	695	39	210	30·8	23·16	20·4
	200	659	80	205	30·4	26·78	27
	400	735	154	228	29·3	31·60	26·4
	600	726	158	226	28·7	32·03	27·0
	800	670	85	218	28·6	27·03	29·7
	1000	620	46	216	29·6	24·08	31·2
20	25	691	51	124	21·8	24·22	20·2
	200	614	80	135	20·5	27·32	27·0
	400	714	169	152	19·7	33·15	25·8
	600	690	142	150	20·0	31·47	27·4
	800	669	113	147	20·0	29·45	28·6
	1000	615	64	143	19·3	25·83	30·5
10	25	691	65	65	10·4	25·37	20·0
	200	595	80	66	9·8	27·63	26·9
	400	692	167	76	9·8	33·52	25·8
	600	674	145	75	9·5	32·09	27·2
	800	668	133	74	9·6	31·22	27·9
	1000	597	69	70	10·0	26·54	30·2
0	25	692	80	0	0	26·59	19·5
	200	593	83	0	0	27·97	26·9
	400	663	152	0	0	32·91	26·1
	600	683	168	0	0	33·82	26·3
	800	667	150	0	0	32·67	27·2
	1000	613	102	0	0	29·45	28·9

the tube. The three components of cutting force F_C, F_T and F_R (Fig. 1) were measured using a specially designed cutting force dynamometer (**9**). The average friction angles λ_n and λ were calculated from these forces using the equation

$$\tan(\lambda_n - \alpha_n) = \frac{F_T}{(F_C{}^2 + F_R{}^2)^{1/2} \sin\left(\tan^{-1}\dfrac{F_R}{F_C} + 90° - i\right)} \quad . \; . \; . \quad (14)$$

which for orthogonal conditions reduces to

$$\tan(\lambda - \alpha) = \frac{F_T}{F_C} \quad . \; . \; . \quad (15)$$

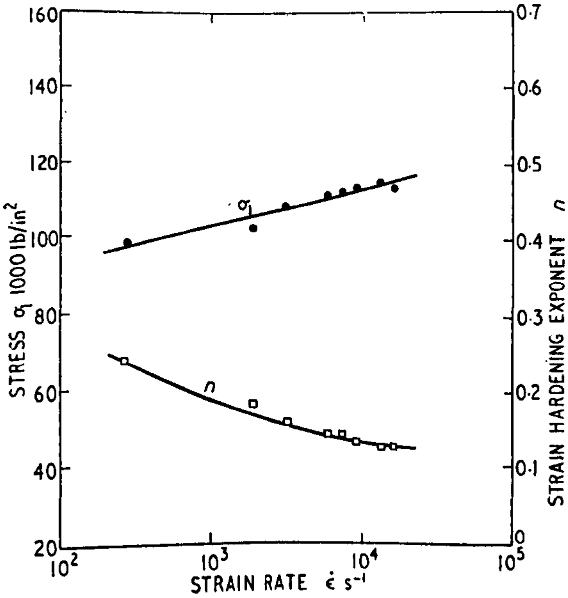

Fig. 3. σ_1 and n values found from orthogonal machining test results

The shear angles ϕ_n and ϕ were calculated using mean chip thickness t_2 ($t'_2 = t_2$) measurements (obtained from an average of 20 readings for each cutting condition) from the equation

$$\tan\phi_n = \tan\phi = \frac{(t_1/t_2)\cos\alpha_n}{1-(t_1/t_2)\sin\alpha_n} \quad . \quad (16)$$

It should be noted that equations (14)–(16) are simply geometric relations derived from Figs 1 and 2. The chip flow direction, defined by the angle η, was measured by observing the wear scar on the cutting face of the tool using a Nikon shadowgraph projector.

5 PREDICTED RESULTS

The theory is now used to predict chip geometry and cutting forces for the same cutting conditions as those in

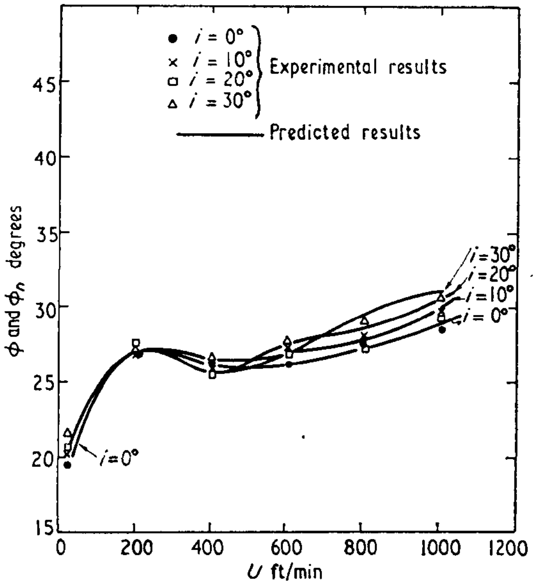

Fig. 4. Predicted and experimental shear angles

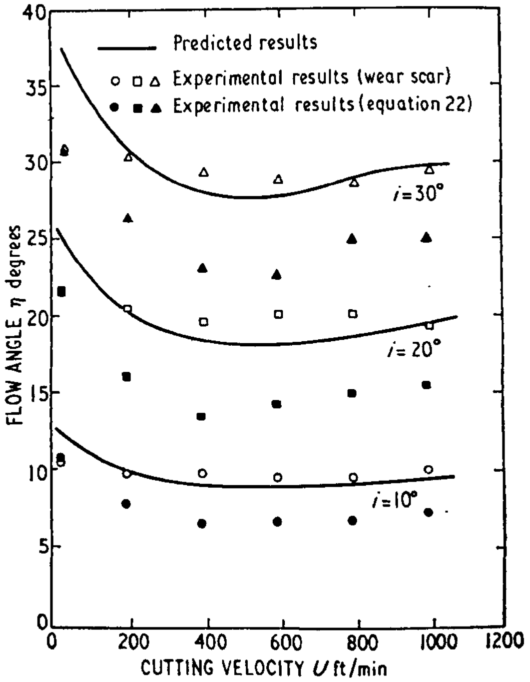

Fig. 5. Predicted and experimental chip flow angles

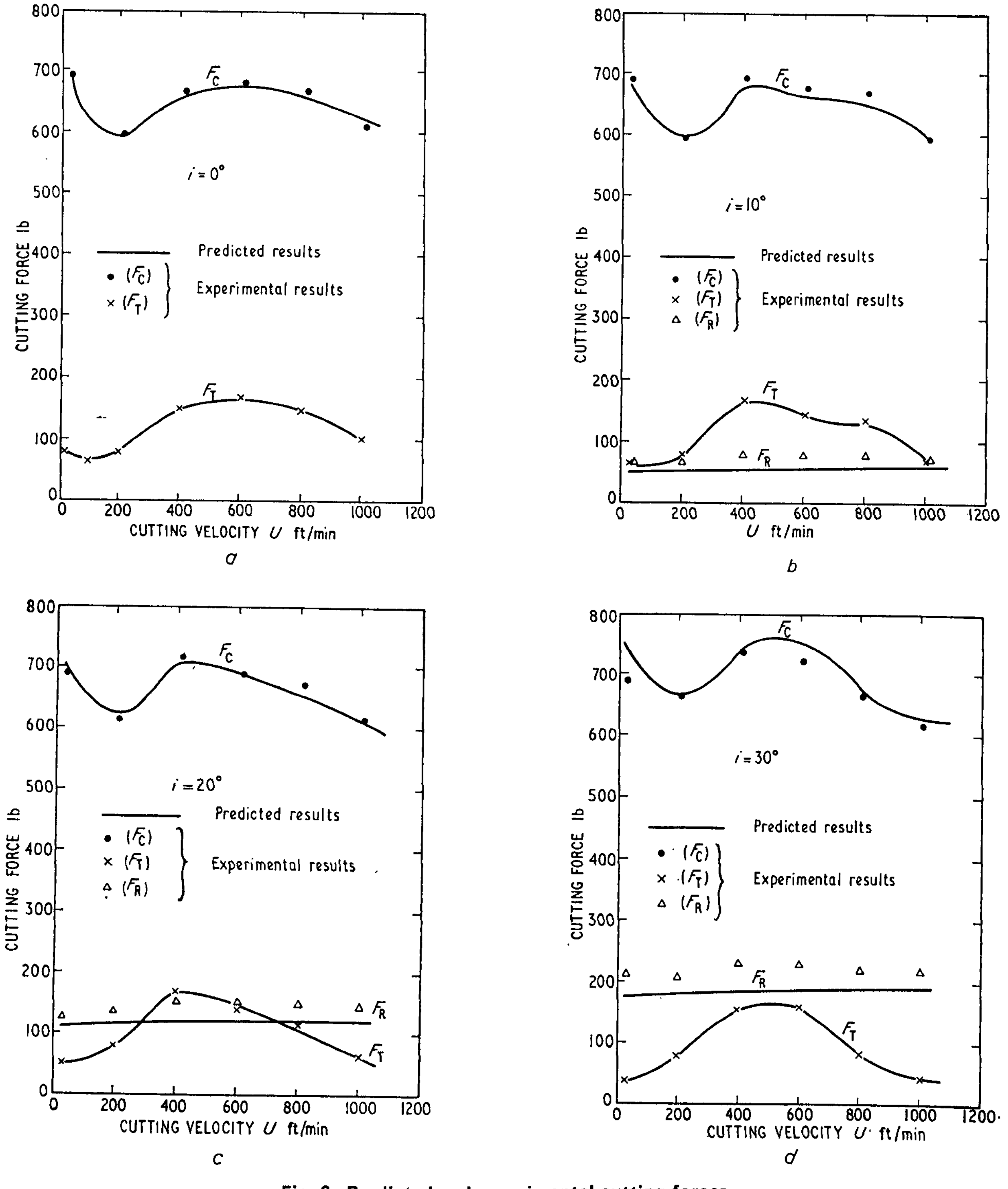

Fig. 6. Predicted and experimental cutting forces

the experiments. The known conditions are taken as being the depth and width of cut t_1 and w, cutting speed U, normal rake angle α_n, inclination angle i and normal friction angle λ_n, together with the appropriate work material properties, i.e. the strain-rate constant C and the flow stress parameters σ_1 and n. It is assumed that σ_1 and n can be represented as functions of strain-rate only for the range of cutting conditions considered although it has been shown (7) that σ_1 in particular is influenced by temperature and account must be taken of this, for example, if the work is preheated or the change in depth of cut is such as to give a large change in temperature.

Lacking independent data for σ_1 and n for the present work material over the ranges of strain-rate and strain of interest the method used is to derive these from the orthogonal machining test results (Table 1) applying the machining theory in reverse. These results are then used with the theory to predict cutting forces etc. for the oblique conditions.

Using the orthogonal experimental values of ϕ and λ

(Table 1) equations (4) and (6) are used to calculate n with the corresponding strain rates ($\dot{\epsilon} = \dot{\gamma}_{AB}/\sqrt{3}$) found from equation (2), C being taken as 5·8 which is the value found in a previous investigation (8) for a similar steel. σ_1 is then found from the equation

$$\sigma_1 = \frac{\sigma_{AB}}{\epsilon_{AB}{}^n} = \frac{\sqrt{3}k_{AB}}{\left(\frac{\gamma_{AB}}{\sqrt{3}}\right)^n} \quad . \quad . \quad . \quad (17)$$

where γ_{AB} is given by equation (3) and k_{AB} is calculated from the experimental shear force F_S (Fig. 2), that is

$$k_{AB} = \frac{F_S \sin \phi}{t_1 w} \quad . \quad . \quad . \quad (18)$$

with F_S given by

$$F_S = (F_C{}^2 + F_T{}^2)^{1/2} \cos \theta \quad . \quad . \quad (19)$$

The values of σ_1 and n found in this way are given in Fig. 3. They show similar trends to those found previously from machining and punching tests (7) (10) for the same kind of steel. For strain rates in the range 10^{-2} to 10^5 s^{-1} the results in Fig. 3 can be represented by the equations

$$\sigma_1 = 73{\cdot}3 + 10{\cdot}1 \log_{10} \dot{\epsilon} \quad . \quad . \quad (20)$$

and

$$n = 0{\cdot}39 + 0{\cdot}000\,001\,6 \log_{10} \dot{\epsilon} - 0{\cdot}04 (\log_{10} \dot{\epsilon})^2 + 0{\cdot}006 (\log_{10} \dot{\epsilon})^3 \quad (21)$$

where the units of σ_1 are 1000 lb/in^2 and the units of $\dot{\epsilon}$ are s^{-1}.

To calculate ϕ_n, η and the three components of cutting force F_C, F_T and F_R for oblique machining the following method is used. For a given set of cutting conditions (i.e. t_1, w, U, α_n, i and λ_n) a reasonable estimate of ϕ_n is made and used with equation (2) to find $\dot{\gamma}_{AB}$ (C is again taken as 5·8). The corresponding value of n is then found from equation (21) and substituted in equation (4) to give θ_n which is used with equation (6) to give λ_n. This process is then repeated with different values of ϕ_n and the value of ϕ_n corresponding to the given value of λ_n found by iteration. Knowing ϕ_n, equation (8) is used to find F'_C and F'_T with k_{AB} having been obtained from equations (3) and (17) using the value of σ_1 obtained from equation (20) for the corresponding strain rate. Equation (10) is then used to calculate η and the forces F_C, F_T and F_R are obtained from equations (12) and (13). Equation (9) is used throughout the calculations to relate uniaxial and plane strain conditions.

Values of ϕ_n, η and cutting forces found in this way are given in Figs 4, 5 and 6. These include the predicted results for $i = 0°$, i.e. orthogonal conditions. The corresponding experimental results are also given.

6 DISCUSSION OF RESULTS

The agreement between the predicted and experimental values of shear angle (Fig. 4) and two of the components of cutting force, i.e. F_C and F_T (Fig. 6), are good. The predicted results also show, in agreement with experiment, that as the inclination angle i is increased the third component of cutting force F_R increases although its value is somewhat underestimated. The experimental values of chip flow angle measured from the wear scar on the tool (Fig. 5) show good agreement with the predicted results for cutting speeds above 200 ft/min. They give an even better fit with equation (1) and it might be expected from this that equation (11), which is derived by substituting equation (1) in equation (10), would give an accurate prediction of ϕ_n. The comparison of experimental values of ϕ_n and equation (11) given in Fig. 7 shows that this is not the case. This suggests that either the method of measuring η from the wear scar is inaccurate or that assumptions made in deriving equation (10) are not valid.

The method of measuring η from the wear scar has been criticized (3) and it has been suggested that more accurate measurements of η can be made by using the measured cutting forces with the equation

$$\tan \eta = \frac{F_C \sin i - F_R \cos i}{(F_C \cos i + F_R \sin i) \sin \alpha_n + F_T \cos \alpha_n} \quad (22)$$

This is derived by assuming that the resultant frictional force on the tool face acts in the direction of chip flow which appears reasonable from physical considerations and which is also one of the assumptions made in deriving equation (10). Values of η found from equation (22) using measured cutting forces are given in Fig. 5 and can be seen to follow the same trend as the predicted results with a marked increase in η at the lower cutting speeds. The theory overestimates η compared with the experimental

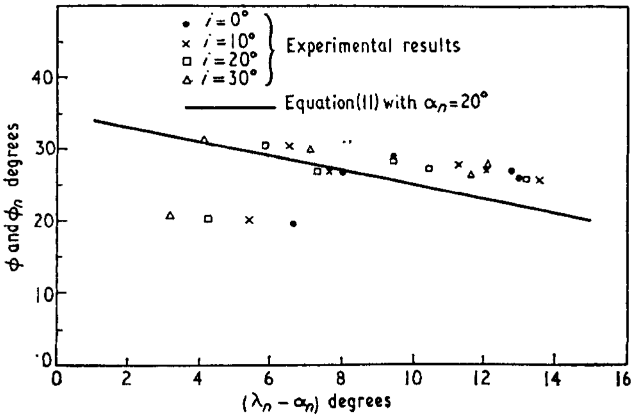

Fig. 7. Comparison of experimental shear angles with equation (11)

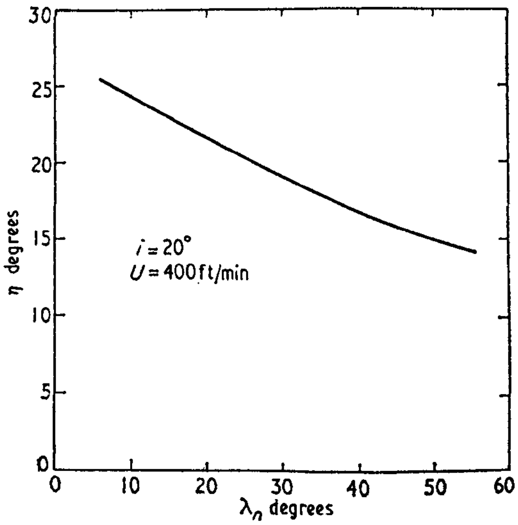

Fig. 8. Predicted increase in η with decrease in λ_n

values found from equation (22) and this is consistent with F_R being underestimated.

The experimental results found from equation (22) show that η can vary even with i and α_n held constant. This has also been shown by experiments (11) in which the friction at the tool–chip interface was varied with all other cutting conditions constant by using a cutting lubricant, a decrease in friction giving a marked increase in η. Equations such as equation (1) in which η is a function of i only and even more elaborate equations which also take account of α_n (3) cannot account for such variations. The predicted results in Fig. 5 show that the present theory is not restricted in this way and that changes in cutting conditions other than i and α_n can change η. In Fig. 8 the theory has been used to calculate the influence of changes in λ_n on η with all other cutting conditions constant. These results show in agreement with experiment (11) that a decrease in λ_n gives an increase in η.

The agreement between experiment and theory is encouraging, particularly when the approximate nature of the theory is considered. A weakness is that λ_n must be known before predictions of cutting forces etc. can be made. λ_n is known from experiment to show large variations with changes in depth of cut, rake angle and cutting speed and can only be measured effectively by machining tests. In a recent analysis of orthogonal machining (4) it was shown how λ_n can be replaced by the shear strength of the chip material at the tool–chip interface as a friction parameter and in this way the predictive value of the theory greatly enhanced. The oblique theory is now being extended in this way.

APPENDIX

REFERENCES

(1) STABLER, G. V. 'The fundamental geometry of cutting tools', *Proc. Instn mech. Engrs* 1951 **165**, 14.

(2) BROWN, R. H. and ARMAREGO, E. J. A. 'Oblique machining with a single cutting edge', *Int. J. Mach. Tool Des. Res.* 1964 **4**, 9.

(3) ARMAREGO, E. J. A. and BROWN, R. H. *The machining of metals* 1969 (Prentice-Hall Inc., Englewood Cliffs, N.J.).

(4) FENTON, R. G. and OXLEY, P. L. B. 'Mechanics of orthogonal machining: allowing for the effects of strain-rate and temperature on tool-chip friction', *Proc. Instn mech. Engrs* 1968–69 **183** (Pt 1), 417–438.

(5) PALMER, W. B. and OXLEY, P. L. B. 'Mechanics of orthogonal machining', *Proc. Instn mech. Engrs* 1959 **173**, 623–651.

(6) ROTH, R. N. and OXLEY, P. L. B. 'Slip-line field analysis for orthogonal machining based upon experimental flow fields', *J. mech. Engng Sci.* 1972 **14** (No. 2), 85.

(7) STEVENSON, M. G. and OXLEY, P. L. B. 'An experimental investigation of the influence of strain-rate and temperature on the flow stress properties of a low carbon steel using a machining test', *Proc. Instn mech. Engrs* 1970–71 **185**, 741.

(8) STEVENSON, M. G. and OXLEY, P. L. B. 'An experimental investigation of the influence of speed and scale on the strain-rate in a zone of intense plastic deformation', *Proc. Instn mech. Engrs* 1969–70 **184** (Pt 1), 561–576.

(9) LIN, G. C. I. and TAYLOR, J. 'Precision measurement of cutting forces', *Proceedings of the 13th M.T.D.R. Conference*, Birmingham University, 1972. (To be published.)

(10) DOWLING, A. R., HARDING, J. and CAMPBELL, J. D. 'The dynamic punching of metals', *J. Inst. Metals* 1970 **98**, 215.

(11) SHAW, M. C., COOK, N. H. and SMITH, P. A. 'The mechanics of three dimensional cutting operations', *Trans. Am. Soc. mech. Engrs* 1952 **74**, 1055.